

Article

A Scent of Peppermint—A Microwave Spectroscopy Analysis on the Composition of Peppermint Oil

Anna Krin ^{1,2}, María Mar Quesada Moreno ^{1,2,†}, Cristóbal Pérez ^{1,2,‡} and Melanie Schnell ^{1,2,*}

¹ Deutsches Elektronen-Synchrotron DESY, Notkestr. 85, 22607 Hamburg, Germany; anna.krin@desy.de (A.K.); mqmoreno@ugr.es (M.M.Q.M.); cristobal.perez@uva.es (C.P.)

² Institute of Physical Chemistry, Christian-Albrechts-Universität zu Kiel, Max-Eyth-Str. 1, 24118 Kiel, Germany
* Correspondence: melanie.schnell@desy.de

† Current address: Departamento de Química Inorgánica, Facultad de Ciencias, Universidad de Granada, Avda. Fuentenueva s/n, 18071 Granada, Spain.

‡ Current address: Departamento de Química Física y Química Inorgánica, Facultad de Ciencias-I.U. CINQUIMA, Universidad de Valladolid, 47011 Valladolid, Spain.

Abstract: Essential oils have a vast number of applications in different areas of our daily life. Detailed chiral analysis and structural characterization of their constituents remains an important subject in analytical chemistry. Here, we report on a broadband rotational spectroscopy study of peppermint oil in the frequency range 2–8 GHz. We focus on an unambiguous determination of the excess enantiomers of the oil constituents menthone and isomenthone in the oil by applying chirality-sensitive rotational spectroscopy, the so-called microwave three-wave mixing (M3WM) technique. Additionally, a new menthol conformer, not previously characterized, was experimentally observed, and the gas-phase structures of the two conformers of menthol and menthone were determined experimentally based on the assignment of their ¹³C-isotopologues in natural abundance.

Keywords: peppermint oil; microwave spectroscopy; substitution structure; microwave three-wave mixing; structural analysis



Citation: Krin, A.; Quesada Moreno, M.M.; Pérez, C.; Schnell, M. A Scent of Peppermint—A Microwave Spectroscopy Analysis on the Composition of Peppermint Oil. *Symmetry* **2022**, *14*, 1262. <https://doi.org/10.3390/sym14061262>

Academic Editor: György Keglevich

Received: 30 April 2022

Accepted: 10 June 2022

Published: 18 June 2022

Publisher's Note: MDPI stays neutral with regard to jurisdictional claims in published maps and institutional affiliations.



Copyright: © 2022 by the authors. Licensee MDPI, Basel, Switzerland. This article is an open access article distributed under the terms and conditions of the Creative Commons Attribution (CC BY) license (<https://creativecommons.org/licenses/by/4.0/>).

1. Introduction

Essential oils of natural origin are complex mixtures containing several structurally similar components, many of which are chiral. Their potential applications in different areas of our daily life are as versatile as their chemical compositions. Nevertheless, like any biologically active substances, they are known to cause not only benefits, but also severe adverse effects when administered in excessive doses [1]. Therefore, it is of common interest to widen our knowledge with respect to these natural resources, which have become indispensable in medicine [2], food industry [3], cosmetics, and even agriculture [4,5].

It was found that the composition of the oils is subject to high variations depending on their origin, chemical treatment, and the method of extraction [6–8]. The enantiomeric excess (ee) of the optically active components of essential oils is often a distinctive feature for the species and the origin of the material used in the production of extracts and oils. Enantiomer differentiation and determination of the respective ee presents a possibility of establishing the authenticity of essential oils [9]. Chiral and chemical analyses thus provide an opportunity to introduce international standards to specify the preferred chemical profile of essential oils with respect to different applications [10]. The possibility to unambiguously differentiate between the enantiomers of a chiral molecule is another key point in the study of essential oils. Many of their constituents are known to be present in enantioenriched form. Since the biological effects of enantiomers can be very different [11,12], the reliable and fast identification of the respective enantiomer in a mixture is important for medical and pharmaceutical purposes.

A number of techniques have been developed over the years to study essential oils. One of the methods of choice is gas chromatography coupled with mass spectrometry (GC-MS) [13]. It is highly suitable for analyzing the composition of mixtures such as essential oils containing volatile components. Substantial technical progress has been achieved over the years with a transition from packed to capillary and further to multidimensional gas chromatography. One of the important milestones is the extension of this technique towards chiral analysis of biologically relevant components. Despite the numerous advantages of this application, some technical issues remain: the preparation of the chiral stationary phase can be laborious and time-consuming. Additionally, many components are too polar or too large to be analyzed with GC-MS. Sometimes, chemical derivatization is required to create sufficiently volatile forms of the compound of interest [14]. In general, it is of advantage to increase the portfolio of available analytical techniques suitable for the analysis of complex mixtures. Another technique that is aimed at studying molecules in the gas phase is broadband rotational spectroscopy. One of its main advantages is the fact that it provides unambiguous signatures of molecular components, even in complex mixtures [15,16]. Since the rotational parameters of molecular species depend on the moments of inertia, and thus on the distribution of atomic masses in the molecule, it is highly sensitive even to only small structural or mass changes. As a consequence, isomers, conformers, and isotopologues exhibit distinct rotational spectra, comparable to a molecular fingerprint. Often, the rotational spectra of ^{13}C isotopologues of the molecules of interest can be recorded in natural abundance, allowing for an accurate structure determination. These powerful features of rotational spectroscopy were exploited and reported in numerous studies [17–21].

A detailed description of the characteristics of broadband rotational spectroscopy is beyond the scope of this manuscript and is provided in several reviews [22–25]. In the context of the present work, it is of importance that rotational spectroscopy complements the information gained from other techniques, for instance, GC-MS. One of the advantages of this technique compared with GC-MS is the ability to differentiate between molecular components of the same mass and very similar structures. Not only does it allow to explore the conformational flexibility of the molecular species of interest, but also to characterize their structural parameters and therefore the respective inter- and intramolecular interactions. The two main requirements are that the molecules of interest need to be polar and that they can be brought into the gas phase, which is the case for the main constituents of essential oils.

Chirality-sensitive rotational spectroscopy, the so-called microwave three-wave mixing (M3WM) technique, provides detailed information on the enantiomers, such as their ee and absolute configuration [26]. Notably, such an information can be retrieved simultaneously for several chiral species, since a M3WM signal can be recorded for specific chiral species without being perturbed by other (chiral) molecules in the sample, as we have for example shown for two conformers of carvone [27]. M3WM is resonant, coherent, and nonlinear, and does not require any chemical or chiral separation, which is often challenging.

Apart from carvone [27], M3WM has been applied to a number of other terpenes and different alcohols such as 1,2-propanediol [28], 1,3-butanediol [28], menthone [29], 4-carvomethenol [30], pulegone [31], solketal [32], and 1-indanol [33]. Additionally, M3WM was reported to be successfully applied on menthone directly in buchu essential oil [16]. In the present work, we characterize the applicability of M3WM in complex mixtures containing several chiral species, without the necessity of any chiral separation or purification prior to the measurement. We chose peppermint essential oil (*Mentha × piperita* L.) as the molecular system for the proof of principle; while some preliminary results on menthone in this essential oil were reported before [34,35], further insights and a detailed analysis of the chiral components of peppermint oil are given here for the first time.

Peppermint oil was investigated in several studies, employing GC-MS and other techniques [36–44]. The main components of this essential oil are menthol and menthone, analyzed using a sensitive gas chromatographic method with flame ionization detector

(GC-FID) and GC-MS [38]. Further components are (+/−)-menthyl acetate, 1,8-cineole, limonene, β -pinene, and β -caryophyllene [38]. As mentioned, the actual chemical composition depends on where the peppermint plants were grown, among other factors. With respect to applications, peppermint oil is known for its antimicrobial [45] and antifungal [46] properties. It has a high concentration of natural pesticides, mainly pulegone and menthone [47]. Peppermint oil is under preliminary research for its potential as a short-term treatment for irritable bowel syndrome [48–50]. Externally, it has been used against muscle and nerve pain [51,52]. High doses of peppermint oil can cause mucosal irritation and mimic episodes of heartburn [53]. As an interesting side note, this oil is also used in construction and plumbing to test for the tightness of pipes and disclose leaks by its characteristic odor.

This manuscript is structured as follows: In the first part, the recorded broadband rotational spectrum of peppermint oil in the 2–8 GHz frequency range will be analyzed. We concentrate here on the main constituents of the oil and their respective conformers. In the next step, we show how we can apply M3WM for a chiral analysis of the oil constituents on the examples of menthone and its diastereomer isomenthone to identify their excess enantiomers. Finally, we use the advantage of high-resolution rotational spectroscopy to determine the structures of menthol and menthone directly in the oil spectrum, based on the assignment of their singly-substituted ^{13}C -isotopologues in natural abundance.

2. Experimental and Computational Techniques

A commercially available sample of peppermint oil was used in the experiment without further purification. The broadband rotational spectrum was recorded using the chirped-pulse Fourier transform microwave (CP-FTMW) spectrometer COMPACT in the frequency range 2–8 GHz. The experimental set-up is presented in detail elsewhere [54,55]. The liquid sample was placed into a custom-made reservoir close to the valve orifice, heated to generate sufficient vapor pressure, and supersonically expanded through a pulsed nozzle (General valve Series 9 operated at 9 Hz) into the gas chamber. Several temperature values ranging from 75 °C to 105 °C were applied to determine optimal heating conditions. The highest signal intensity was observed by heating the sample at 90 °C. Neon was used as a carrier gas (3 bar backing pressure). The “fast frame” option of the digital oscilloscope was used to reduce the measurement time and the sample consumption [21]. Eight back-to-back excitation chirps were performed per gas pulse, giving an effective repetition rate of 72 Hz. All FID acquisitions were co-added and averaged, resulting in a total of 4 million averages. Fast Fourier transformation of the FIDs from the time into the frequency domain was performed to obtain the final rotational spectrum.

To facilitate the analysis of menthol, the major constituent of peppermint oil, a separate broadband measurement on commercially available menthol (Sigma Aldrich, 99% purity) was carried out in the 2–8 GHz frequency range. The procedure of obtaining the spectrum resembles the one described above. The sample was heated to 75 °C, and the neon backing pressure was 3 bar. In total, 4.3 million averages were co-added to obtain the final spectrum.

Rotational transitions were fitted to an asymmetric rigid rotor Hamiltonian, using the JB95 [56] and PGOPHER [57] program packages. Refined fits were obtained using Watson’s A-reduced rigid rotor Hamiltonian in the I' representation as implemented in the SPFIT program developed by Pickett [58].

Structures of the two conformers belonging to menthol and menthone were optimized with the software package ORCA [59,60] at the B3LYP level of theory with Grimme’s empirical dispersion correction [61] and the def2-TZVPP basis set to compare the computational prediction with the experimental results (Section 3.4). Frequency calculations were carried out to ensure that the structures were true minima and to obtain their zero-point-corrected relative energies.

3. Results and Discussion

3.1. The Broadband Rotational Spectrum and Identified Components

The recorded broadband rotational spectrum is very dense (Figure 1). Several peppermint oil constituents were analyzed in previous rotational spectroscopy studies and identified in the present spectrum based on their experimental rotational parameters. These components are: menthol EQ1ext [62], menthone A [62], menthone B [62], menthone C [62], isomenthone-eq-ax A [62], pulegone Chair 1 [31], menthyl acetate m_eq 1 [63], isopulegol conformer 1 [64], isopulegol conformer 2 [64], limonene EQ1 [65], α -pinene [66], β -pinene [67], and eucalyptol [68]. The respective reported rotational parameters are summarized in Table 1. Note that the nomenclature used here corresponds to the one applied in the respective study, the additional information in the name refers to the respective conformer(s).

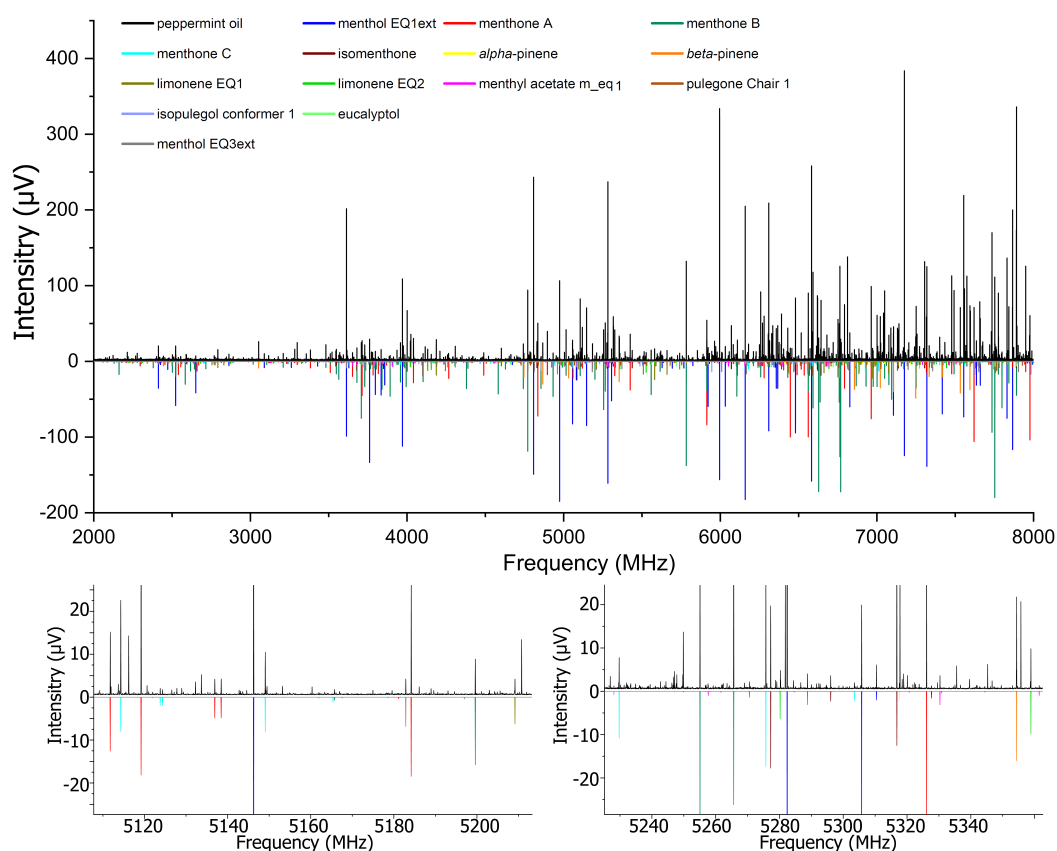


Figure 1. The broadband rotational spectrum (4 million acquisitions, neon as a carrier gas) of peppermint oil in the 2–8 GHz frequency range. The black trace shows the experimental spectrum, while the lower traces represent simulations based on previously reported (see text) rotational parameters for the main constituents of peppermint oil. The two lower panels show zoomed-in spectra for better visibility. Note that, in the zoomed-in spectra, some of the stronger transitions are cut in intensity.

Menthol EQ1ext is the strongest species in the spectrum with a signal-to-noise ratio (SNR) of about 1200:1 for the strongest transitions. In the previous rotational spectroscopy study on menthol [62], several low-energy conformers were predicted at the MP2/6-311++G(d,p) level of theory. Based on these results, another menthol conformer, EQ3ext, was experimentally assigned in the pure menthol broadband rotational spectrum, which was not previously identified, and subsequently analyzed in the peppermint oil spectrum. The procedure is explained in detail in Section 3.2. The SNR of this higher-energy conformer, EQ3ext, in the peppermint oil spectrum is 50:1.

The next strongest species after menthol EQ1ext are the two menthone conformers menthone B (SNR 700:1) and menthone A (460:1), followed by isomenthone-eq-ax A (300:1), menthone C (185:1), β -pinene (127:1), eucalyptol (110:1), limonene EQ1 (50:1), isopulegol 1 (37:1), and menthyl acetate m_eq 1 (35:1). Other identified species (pulegone Chair 1, isopulegol 2, α -pinene) were weaker with an SNR of about 10:1.

Note that the preliminary results of our rotational spectroscopy study on peppermint oil reported before [35] were obtained for a different sample of this essential oil, and eucalyptol was observed to be the most intense species in the spectrum, emphasizing the previously discussed difference in the chemical composition of the two oils.

Table 1. Experimental rotational constants and calculated magnitudes of the permanent electric dipole moment components for the peppermint oil constituents identified in the broadband rotational spectrum. The calculated values for the dipole moment components and zero-point-corrected relative energies were determined at the levels of theory reported in the respective original work.

| Component | A (MHz) | B (MHz) | C (MHz) | $ \mu_a $ (D) | $ \mu_b $ (D) | $ \mu_c $ (D) | ΔE^e (kJ/mol) | Ref. |
|------------------------|------------------|-----------------|-----------------|------------------|---------------|---------------|-----------------------|------|
| Menthol EQ1ext | 1779.79549(38) | 692.62171(24) | 573.34542(27) | 1.4 ^a | 0.1 | 0.8 | 0 | [62] |
| Menthol EQ3ext | 1962.36595(77) | 672.28085(29) | 579.65418(31) | 1.6 ^a | 0.03 | 0.8 | 3.3 | – |
| Menthone A | 1953.43379(43) | 694.51551(19) | 586.57758(19) | 1.2 ^a | 2.5 | 0.5 | 0.8 | [62] |
| Menthone B | 2021.98637(36) | 693.53686(16) | 562.13636(16) | 1.2 ^a | 2.2 | 1.2 | 0.0 | [62] |
| Menthone C | 2109.38469(65) | 681.13604(27) | 598.12413(25) | 1.6 ^a | 2.0 | 1.2 | 3.9 | [62] |
| Isomenthone | 1535.27577(48) | 812.92526(33) | 671.43466(33) | 0.6 ^a | 2.9 | 1.0 | 0.0 | [62] |
| Menthyl acetate m_eq 1 | 687.63788(34) | 577.21454(14) | 357.20440(19) | 0.5 ^a | 0.9 | 1.4 | 0.0 | [63] |
| α -Pinene | 1936.55844(14) | 1228.635670(76) | 1127.020991(77) | 0.1 ^a | 0.1 | 0.04 | 0.0 | [66] |
| β -Pinene | 1901.889140(175) | 1293.661042(80) | 1150.831087(81) | 0.5 ^a | 0.6 | 0.1 | 0.0 | [67] |
| Limonene EQ 1 | 3058.01643(149) | 717.04590(76) | 679.25973(75) | 0.4 ^c | 0.4 | 0.4 | 0.0 | [65] |
| Eucalyptol | 1545.88814(51) | 1080.46796(37) | 1038.93323(32) | 0.0 ^b | 1.6 | 0.0 | 0.0 | [68] |
| Pulegone Chair 1 | 1909.05435(71) | 739.06297(21) | 578.14181(21) | 0.7 ^a | 2.7 | 1.0 | 0.0 | [31] |
| Isopulegol 1 | 1949.96485(299) | 700.16883(113) | 591.63903(111) | 0.4 ^d | 2.0 | 0.5 | 0.0 | [64] |
| Isopulegol 2 | 1914.31605(195) | 702.84904(119) | 578.53932(124) | 0.5 ^d | 1.8 | 0.5 | 3.7 | [64] |

^a MP2/6-311++G(d,p); ^b MP2/cc-pVTZ; ^c MP2/6-311++G(2df,p); ^d M06-2X/6-311++G(d,p); ^e Zero-point corrected relative energies.

3.2. Menthol Conformers

The conformational landscape of several peppermint oil components is very rich. In a previously reported study on menthol [62], five of its conformers with zero point corrected relative energies up to 5 kJ/mol were determined computationally. These are EQ1ext, EQ1int2, EQ1int, EQ3ext, and EQ3int; based on the nomenclature used by Schmitz et al. [62], EQ1ext is the lowest energy conformer, which was also identified in our recorded peppermint oil broadband rotational spectrum, as described in Section 3.1. EQ1ext, EQ1int, and EQ1int2 differ in the orientation of the hydroxyl group with an interconversion barrier of about 1 kJ/mol (B3LYP/6-311++G(d,p)) [62]. Therefore, it is expected that the conformers EQ1int2 and EQ1int relax to EQ1ext under the supersonic conditions of our molecular jet.

To facilitate the assignment of the other menthol conformers, a separate broadband rotational spectrum of pure menthol was recorded (2–8 GHz, SNR 3500:1 for the strongest transitions of menthol EQ1ext). This allowed us to assign an additional, previously unobserved menthol conformer (Table S7 in Supplementary) that was subsequently identified in the peppermint oil broadband rotational spectrum.

A comparison between the experimentally determined conformer 2 and theoretical rotational parameters (MP2/6-311++G(d,p) level of theory) of EQ3int and EQ3ext is pre-

sented in Table 2. Conformers EQ3int and EQ3ext are structurally similar and differ only in the orientation of the hydroxyl group [62]. The calculated rotational constants B and C of these conformers are similar, while there is a difference in their A rotational constant of about 15 MHz. As evident from Table 2, the rotational constant A of conformer 2 is closer to the one of EQ3int.

Table 2. Comparison between the computationally determined molecular parameters for EQ3ext and EQ3int (MP2/6-311++G(d,p) level of theory) and the experimentally obtained ones (conformer 2). The calculated parameters were taken from Schmitz et al. [62], while the experimental ones belong to the species assigned in the broadband rotational spectrum of menthol. Information about the observation of the different types of rotational transitions a, b, and c, which depend on the dipole moment components μ_a , μ_b , and μ_c , is provided for conformer 2 (y—observed; n—not observed).

| Parameter | Experimental Conformer 2 | MP2 ^{ab} | |
|--------------------------|-----------------------------|---------------------|---------------------|
| | | EQ3ext ^b | EQ3int ^b |
| A MHz | 1962.47014(36) | 1975 | 1960 |
| B MHz | 672.28148(25) | 674.7 | 674.1 |
| C MHz | 579.65712(28) | 582.7 | 581.5 |
| ΔJ kHz | 0.0283(40) | | |
| μ_a D ^c | y | 1.6 | 1.1 |
| μ_b D | n | −0.03 | −1.0 |
| μ_c D | y | 0.8 | −0.9 |
| ΔE^d kJ/mol | | 3.0 | 5.0 |
| σ^e kHz | 4.6 | | |
| N ^f | 50 | | |

^a 6-311++G(d,p); ^b Parameters and nomenclature of the conformers taken from Ref. [62]; ^c dipole moment components; ^d zero-point-corrected relative energies; ^e RMS deviation of the fit; ^f number of fitted transitions.

An additional parameter for guiding the assignment are the calculated dipole moment components. For EQ3int, the three dipole moment components μ_a , μ_b , and μ_c have a value of approximately 1 D, while μ_b is close to zero for EQ3ext. It means that for EQ3int all three types of rotational transitions are expected to be observed in the rotational spectrum, while for EQ3ext only a- and c-type transitions should be observable. Only a- and c-type transitions could be assigned in our spectrum, meaning that the second experimentally observed conformer of menthol is indeed EQ3ext. Another aspect corroborating the assignment is the zero-point-corrected relative energy, which is lower for EQ3ext in comparison with EQ3int (see Table 2). Summarizing all the aspects, the second menthol conformer observed in the spectrum can be assigned as EQ3ext.

3.3. Enantiomer Differentiation Using M3WM

Once a broad overview of the oil constituents and their conformers was gained, we performed a chiral analysis on some of the components, which will be discussed in the present section. Many of the peppermint oil constituents are chiral and can be expected to occur enantioenriched because of the natural origin of the essential oil. From an analytic point of view, the analysis of such a sample can be challenging, despite being a common situation in many areas of chemistry. As discussed above, M3WM relies on the high-resolution fingerprint character of rotational spectroscopy. It is based on the fact that the scalar triple product of the dipole-moment components μ_a , μ_b , and μ_c has an opposite sign for the two enantiomers. A three-level system consisting of three rotational dipole-allowed transitions—which depend on the dipole moment components μ_a , μ_b , and μ_c , respectively—is needed for the M3WM experiment. By resonantly exciting two of the rotational transitions with orthogonally polarized microwave fields, a signal containing chiral information is recorded as an FID in the third mutually orthogonal direction. The two excitation pulses are called “drive” and “twist”, while the recorded signal is referred to as “listen”. The intensity of the recorded listen signal is directly proportional to the enantiomeric excess (ee). A non-zero signal is only observed once one of the enantiomers is

in excess. To accurately determine the ee value, a normalization of the signal amplitude with that of a sample with a known ee (reference) is required [29]. The information about the handedness of the chiral species is encoded in the phase of the recorded signal.

According to the literature [37], the major peppermint oil components have the following excess enantiomers: (–)-menthol, (–)-menthone, and (+)-isomenthone. Chiral analysis of these monoterpenes directly in the oils is an opportunity to benchmark the M3WM technique and to show its applicability in complex mixtures that contain chemically and structurally (i.e., stereoisomers, conformers) similar components. A prerequisite for M3WM is that all three dipole-moment components of the chiral species are non-zero. This is usually the case for C_1 -symmetric chiral molecules containing a stereogenic center. However, due to a special geometric arrangement, such as in the case of menthol or camphor [69], one or more of the three dipole moment components can become close to or equal to zero. Therefore, M3WM could not be performed on the two conformers of menthol EQ1ext and EQ3ext, where μ_b is close to zero. Instead, the measurement was carried out on menthone A and isomenthone-eq-ax A, for which we successfully applied M3WM before, using pure samples [29,70].

The respective M3WM cycles and the obtained chiral signals in form of the FID of the listen transition are displayed in Figure 2. In case of menthone A, the same cycle was used as reported by Schmitz et al. [29]. The applied pulse durations of the drive and twist pulses were optimized in previous M3WM experiments [71]. For isomenthone, a new cycle was chosen here, which involves the same rotational energy levels defined by the rotational quantum numbers $J_{K_a K_c}$ as the cycle used for menthone A (Figure 2). An optimal pulse duration of the drive was determined by monitoring the intensity of the transition at 3974.05 MHz, while changing the pulse duration from 0 to 200 ns in steps of 25 ns. For the twist, the intensity of the isomenthone listen transition at 3549.59 MHz was monitored, while tuning the twist pulse from 0 to 3700 ns in steps of 50 ns, i.e., using a double-resonance arrangement. The highest listen signal intensity of isomenthone was obtained with the drive pulse of 100 ns and the twist of 3700 ns duration. These results are summarized in Figure 2.

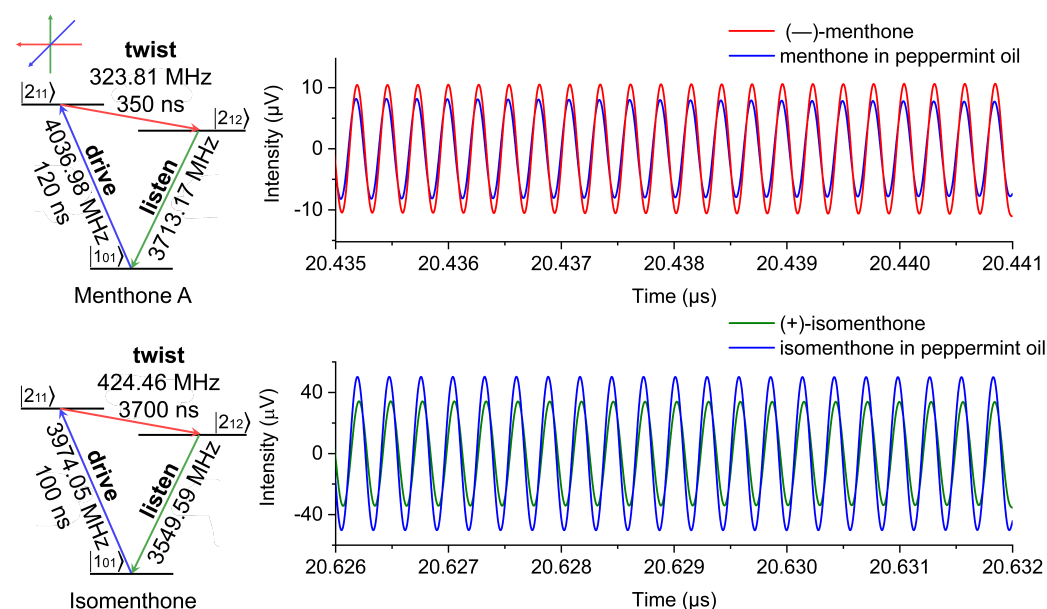


Figure 2. Left: Microwave three-wave mixing (M3WM) cycles for menthone A and isomenthone eq-ax with the respective optimized pulse durations of the drive and the twist transitions. Right: Time-domain results (FIDs) of the listen transition for menthone and isomenthone both in peppermint oil and in commercially available enantioenriched samples containing either (–)-menthone or (+)-isomenthone.

To identify the absolute configuration of menthone and isomenthone in peppermint oil, commercially available enantioenriched samples of known handedness ((+)-menthone, 90% purity, (−)-menthone, 90% purity, (+)-isomenthone, 90% purity) were used as a reference. The time-domain results for both listen transitions of menthone and isomenthone are presented in Figure 2. In the case of menthone, the phases of the FIDs of the listen transitions in the time domain are in phase for the enantioenriched (−)-menthone A and menthone A in the oil, identifying (−)-menthone as the enantiomer in excess in the oil. For isomenthone, there is an evident phase match between the time-domain signal of (+)-isomenthone used as a reference and isomenthone present in the oil. These results are in agreement with the published analytical data on the chiral composition of peppermint oil (*Mentha* species) and demonstrate the applicability of M3WM to complex chiral samples. The exact ee values for menthone and isomenthone were not determined here, but a main focus was placed on the determination of the handedness of the excess enantiomer.

3.4. Experimental Structures of the Oil Constituents

Here, the structural analysis of the two oil components, menthol EQ1ext and menthone B, is described. This analysis is also an illustration of the power of broadband rotational spectroscopy for a comprehensive analysis of complex mixtures from different analytical points of view. The determined rotational parameters for the isotopic species of menthol EQ1ext and menthone B are summarized in Tables S1 and S4 (in Supplementary). The information given there allowed us to obtain the experimental structures of the respective species using different established approaches.

One of the methods is based on solving the so-called Kraitchman's Equations [72]. This approach is mostly used for species with only single isotopic substitutions. The respective structure obtained is commonly referred to as r_s . It is determined atom-by-atom by calculating the differences in the moments of inertia between the parent and the isotopologue. In principle, no input from the theoretical models is required for determining the atomic coordinates. However, there are some known drawbacks of this method. For instance, only the magnitudes of the atomic coordinates are obtained. The signs have to be determined by other means, e.g., from quantum chemical results or by comparison with experimental results for similar molecular systems. Additionally, the method fails for the atoms located in the proximity to the principal axes, where the calculated differences in moments of inertia are close to zero. This results in imaginary numbers for one or several atomic coordinates (see Tables S2 and S5 in Supplementary), which subsequently have to be fixed to zero. For instance, in menthone B some of the coordinates of C2 (close to the y-axis, see Figure 3), C4 (close to the y-axis), and C11 (x-y plane) were set to zero.

There are several alternative methods to refine the experimentally determined structure. One of them allowed us to calculate the effective ground-state r_0 structure by fitting structural parameters directly to the observed isotopic moments of inertia in a nonlinear least-squares procedure. This method has an advantage of also exploiting multi-isotopic substitution. However, in contrast to the Kraitchman approach, a set of constraints from quantum chemical calculations might be required for the determination of structural parameters, depending on the analyzed molecular system.

Both substitution (r_s) and effective (r_0) structures were determined for menthol EQ1ext and menthone B from the assignments of the respective isotopologues directly in the peppermint oil spectrum. The overall standard deviations of the r_0 -fit were 0.011 u^2 and 0.030 u^2 for EQ1ext and menthone B, respectively. A comparison between the results obtained with r_s and r_0 fits is presented in Figure 3.

A theoretical prediction of the respective equilibrium structures (r_e) was obtained at the B3LYP/def2-TZVPP level of theory for both molecular systems. The experimental structural parameters (r_s and r_0) are compared with the ones of the equilibrium structure and presented in Tables S3 and S6 (in Supplementary). In general, a good agreement between theory and experiment is evident. For some structural parameters, the theoretical predictions match the experimental results of the r_0 better compared to the r_s . This is for

instance the case for the distances C4–C5, C8–C11, and the angles $\angle(C2 - C3 - C4)$ and $\angle(C4 - C5 - C6)$ of menthone B (Table S6). In these cases, one or several atoms are close to a principal axis.

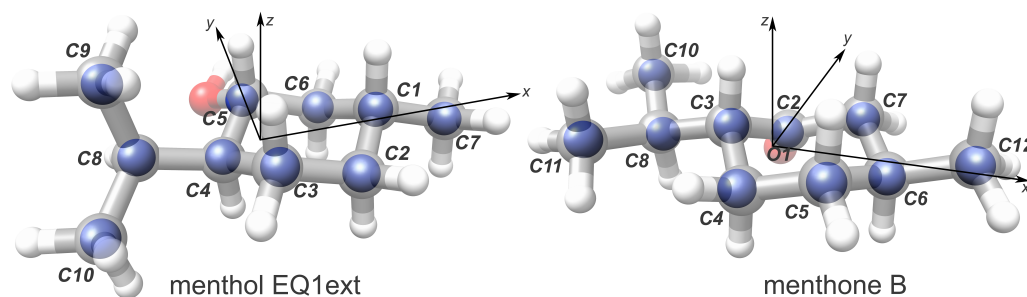


Figure 3. Comparison between the r_0 -structure (ball-and-stick representation) and the Kraitchman structure r_s (blue spheres) for menthol EQ1ext and menthone B obtained from the assignment of the ^{13}C isotopologues directly in peppermint oil. The three principal axes $-x, y,$ and $z-$ are depicted.

4. Conclusions

Different molecular species present in a commercially available sample of peppermint oil have been identified in the broadband rotational spectrum in spite of their structural similarity. Moreover, the respective conformational and diastereomeric forms of the oil constituents were assigned. Diastereomers differ in their structures and can therefore be distinguished by rotational spectroscopy due to their unique rotational spectra. The lowest-energy conformer of menthol, EQ1ext, is the strongest species in the spectrum, followed by the menthone B conformer. Their singly substituted ^{13}C isotopologues in natural abundance were assigned directly in the peppermint oil spectrum, which allowed us to obtain accurate structures. The analysis of the broadband rotational spectrum of pure menthol revealed the presence of an additional conformer of menthol not characterized previously, EQ3ext. This conformer was subsequently identified in the peppermint oil broadband spectrum as well. The results demonstrate the power of broadband rotational spectroscopy as an analytical tool to disentangle a complex composition of biologically relevant samples, including structure determination.

The main highlight of the present work is a chirality-sensitive analysis on two chiral species in peppermint oil, a complex mixture of several chiral components. Here, we performed M3WM on menthone and its diastereomer isomenthone directly in the oil and showed how M3WM can be applied to determine the chirality of the excess enantiomers in mixtures without the necessity of prior separation or purification of the molecules of interest, since the molecular signal is not perturbed by the simultaneous presence of other chiral species in the sample.

Supplementary Materials: The following supporting information can be downloaded at: <https://www.mdpi.com/article/10.3390/sym14061262/s1>, Table S1: Experimentally determined rotational constants for the isotopic species of menthol EQ1ext; Table S2: Experimental and calculated atomic coordinates of menthol EQ1ext; Table S3: Experimental and calculated structural parameters of menthol EQ1ext; Table S4: Experimentally determined rotational constants for the isotopic species of menthone B; Table S5: Experimental and calculated atomic coordinates of menthone B; Table S6: Experimental and calculated structural parameters of menthone B; Table S7: Measured rotational transitions and the residuals of menthol EQ3ext.

Author Contributions: Conceptualization, A.K., C.P. and M.S.; formal analysis, A.K., C.P. and M.M.Q.M.; writing—original draft preparation, A.K. and M.M.Q.M.; writing—review and editing M.S.; supervision, M.S. All authors have read and agreed to the published version of the manuscript.

Funding: This work has been funded by the Deutsche Forschungsgemeinschaft (DFG, Projektnummer 328961117 SFB 1319 ELCH). M.M.Q.M. thanks Fundación Alfonso Martín Escudero for a postdoctoral

grant and Ministerio de Ciencia, Innovación y Universidades for a Juan de la Cierva formación contract (grant FJC2018-035709-I supported by MCIN/AEI10.13039/501100011033).

Institutional Review Board Statement: Not applicable.

Informed Consent Statement: Not applicable.

Data Availability Statement: Not applicable.

Acknowledgments: This research was supported in part through the Maxwell computational resources operated at Deutsches Elektronen-Synchrotron DESY, Hamburg, Germany.

Conflicts of Interest: The authors declare no conflict of interest.

References

1. Vostinaru, O.; Heghes, S.C.; Filip, L. Safety Profile of Essential Oils. In *Essential Oils*; IntechOpen: Rijeka, Croatia, 2020. [CrossRef]
2. Bakkali, F.; Averbeck, S.; Averbeck, D.; Idaomar, M. Biological effects of essential oils—A Review. *Food Chem. Toxicol.* **2008**, *46*, 446–475. [CrossRef]
3. Mihai, A.; Popa, M. Essential oils utilization in food industry—A literature review. *Sci. Bull. Ser. F Biotechnol.* **2013**, *17*, 187–192.
4. Zanellato, M.; Masciarelli, E.; Boccia, P.; Sturchio, E.; Pezzella, M.; Cavalieri, A.; Caporali, F. The essential oils in agriculture as an alternative strategy to herbicides: A case study. *Int. J. Environ. Health* **2009**, *3*, 198–213. [CrossRef]
5. Tripathi, A.K.; Upadhyay, S.; Bhuyan, M.; Bhattacharya, P.R. A review of essential oils as biopesticide in insect-pest management. *J. Pharmacogn. Phytother.* **2009**, *15*, 52–53.
6. Zouari, N.; Ayadi, I.; Fakhfakh, N.; Rebai, A.; Zouari, S. Variation of chemical composition of essential oils in wild populations of *Thymus algeriensis* Boiss. et Reut., a North African endemic Species. *Lipids Health. Dis.* **2012**, *11*, 28. [CrossRef]
7. Barra, A. Factors Affecting Chemical Variability of Essential Oils: A Review of Recent Developments. *Nat. Prod. Commun.* **2009**, *4*, 1147–1154. [CrossRef]
8. Figueiredo, A.; Barroso, J.; Pedro, L.; Scheffer, J. Factors affecting secondary metabolite production in plants: Volatile components and essential oils. *Flavour Fragr. J.* **2008**, *23*, 213–226. [CrossRef]
9. Castillo, M.; Blanch, G.; Herraiz, M. Natural variability of the enantiomeric composition of bioactive chiral terpenes in *Mentha piperita*. *J. Chromatogr. A* **2004**, *1054*, 87–93. [CrossRef]
10. Sadgrove, N.; Jones, G. A Contemporary Introduction to Essential Oils: Chemistry, Bioactivity and Prospects for Australian Agriculture. *Agriculture* **2015**, *5*, 48–102. [CrossRef]
11. Brookes, J.C.; Horsfield, A.P.; Stoneham, A.M. Odour character differences for enantiomers correlate with molecular flexibility. *J. R. Soc. Interface* **2009**, *6*, 75–86. [CrossRef]
12. Nguyen, L.; He, H.; Pham-Huy, C. Chiral Drugs: An Overview. *Int. J. Biomed. Sci.* **2006**, *2*, 85–100.
13. Cazaussus, A.; Pes, R.; Sellier, N.; Tabet, J.C. GC-MS and GC-MS-MS analysis of a complex essential oil. *Chromatographia* **1988**, *25*, 865–869. [CrossRef]
14. Rockwood, A.L.; Kushnir, M.M.; Clarke, N.J. 2—Mass Spectrometry. In *Principles and Applications of Clinical Mass Spectrometry*; Rifai, N., Horvath, A.R., Wittwer, C.T., Eds.; Elsevier: Amsterdam, The Netherlands, 2018; pp. 33–65. [CrossRef]
15. Quesada-Moreno, M.M.; Krin, A.; Schnell, M. Analysis of thyme essential oils using gas-phase broadband rotational spectroscopy. *Phys. Chem. Chem. Phys.* **2019**, *21*, 26569–26579. [CrossRef]
16. Pate, B.H.; Evangelisti, L.; Caminati, W.; Xu, Y.; Thomas, J.; Patterson, D.; Perez, C.; Schnell, M. Chapter 17—Quantitative Chiral Analysis by Molecular Rotational Spectroscopy. In *Chiral Analysis*, 2nd ed.; Polavarapu, P.L., Ed.; Elsevier: Amsterdam, The Netherlands, 2018; pp. 679–729. [CrossRef]
17. Domingos, S.R.; Pérez, C.; Medcraft, C.; Pinacho, P.; Schnell, M. Flexibility unleashed in acyclic monoterpenes: Conformational space of citronellal revealed by broadband rotational spectroscopy. *Phys. Chem. Chem. Phys.* **2016**, *18*, 16682–16689. [CrossRef]
18. Macario, A.; Blanco, S.; Thomas, J.; Xu, Y.; López, J. The Conformational Landscape of *m*-Anisic Acid and Its Complexes with Formic Acid. *J. Phys. Chem. A* **2019**, *123*, 6772–6780. [CrossRef]
19. Tubergen, M.J.; Conrad, A.R.; Chavez, R.E.; Hwang, I.; Suenram, R.D.; Pajski, J.J.; Pate, B.H. Gas-phase conformational distributions for the 2-alkylalcohols 2-pentanol and 2-hexanol from microwave spectroscopy. *J. Mol. Spectrosc.* **2008**, *251*, 330–338. [CrossRef]
20. Pérez, C.; Muckle, M.T.; Zaleski, D.P.; Seifert, N.A.; Temelso, B.; Shields, G.C.; Kisiel, Z.; Pate, B.H. Structures of Cage, Prism, and Book Isomers of Water Hexamer from Broadband Rotational Spectroscopy. *Science* **2012**, *336*, 897–901. [CrossRef]
21. Pérez, C.; Lobsiger, S.; Seifert, N.A.; Zaleski, D.P.; Temelso, B.; Shields, G.C.; Kisiel, Z.; Pate, B.H. Broadband Fourier transform rotational spectroscopy for structure determination: The water heptamer. *Chem. Phys. Lett.* **2013**, *571*, 1–15. [CrossRef]
22. Schnell, M. Broadband Rotational Spectroscopy for Molecular Structure and Dynamics Studies. *Z. Phys. Chem.* **2013**, *227*, 1–22. [CrossRef]
23. Xu, Y.; Jäger, W. Microwave Rotational Spectroscopy. In *Encyclopedia of Inorganic and Bioinorganic Chemistry*; American Cancer Society: Atlanta, GA, USA, 2011. [CrossRef]
24. Morino, Y.; Hirota, E. Microwave Spectroscopy. *Annu. Rev. Phys. Chem.* **1969**, *20*, 139–166. [CrossRef]

25. Park, G.; Field, R. Perspective: The first ten years of broadband chirped pulse Fourier transform microwave spectroscopy. *J. Chem. Phys.* **2016**, *144*, 200901. [[CrossRef](#)] [[PubMed](#)]
26. Patterson, D.; Schnell, M.; Doyle, J.M. Enantiomer-specific detection of chiral molecules via microwave spectroscopy. *Nature* **2013**, *497*, 475–478. [[CrossRef](#)] [[PubMed](#)]
27. Shubert, V.A.; Schmitz, D.; Patterson, D.; Doyle, J.M.; Schnell, M. Identifying Enantiomers in Mixtures of Chiral Molecules with Broadband Microwave Spectroscopy. *Angew. Chem. Int. Ed.* **2014**, *53*, 1152–1155. [[CrossRef](#)] [[PubMed](#)]
28. Patterson, D.; Doyle, J.M. Sensitive Chiral Analysis via Microwave Three-Wave Mixing. *Phys. Rev. Lett.* **2013**, *111*, 023008. [[CrossRef](#)]
29. Alvin Shubert, V.; Schmitz, D.; Schnell, M. Enantiomer-sensitive spectroscopy and mixture analysis of chiral molecules containing two stereogenic centers—Microwave three-wave mixing of menthone. *J. Mol. Spectrosc.* **2014**, *300*, 31–36. Spectroscopic Tests of Fundamental Physics, [[CrossRef](#)]
30. Shubert, V.; Schmitz, D.; Medcraft, C.; Krin, A.; Patterson, D.; Doyle, J.; Schnell, M. Rotational spectroscopy and three-wave mixing of 4-carvomethenol: A technical guide to measuring chirality in the microwave regime. *J. Chem. Phys.* **2015**, *142*, 214201. [[CrossRef](#)]
31. Krin, A.; Pérez, C.; Pinacho, P.; Quesada-Moreno, M.M.; López-González, J.J.; Avilés-Moreno, J.R.; Blanco, S.; López, J.C.; Schnell, M. Structure Determination, Conformational Flexibility, Internal Dynamics, and Chiral Analysis of Pulegone and Its Complex with Water. *Chem. Eur. J* **2018**, *24*, 721–729. [[CrossRef](#)]
32. Lobsiger, S.; Pérez, C.; Evangelisti, L.; Lehmann, K.; Pate, B. Molecular Structure and Chirality Detection by Fourier Transform Microwave Spectroscopy. *J. Phys. Chem. Lett.* **2014**, *6*, 196–200. [[CrossRef](#)]
33. Lee, J.; Bischoff, J.; Hernandez-Castillo, A.; Sartakov, B.; Meijer, G.; Eibenberger-Arias, S. Quantitative study of enantiomer-specific state transfer. *Phys. Rev. Lett.* **2021**, *128*, 173001. [[CrossRef](#)]
34. Shubert, V.; Schmitz, D.; Pérez, C.; Medcraft, C.; Krin, A.; Domingos, S.; Patterson, D.; Schnell, M. Chiral Analysis Using Broadband Rotational Spectroscopy. *J. Phys. Chem. Lett.* **2015**, *7*, 341–350. [[CrossRef](#)]
35. Domingos, S.; Pérez, C.; Schnell, M. Sensing Chirality with Rotational Spectroscopy. *Annu. Rev. Phys. Chem.* **2018**, *69*, 499–519. [[CrossRef](#)] [[PubMed](#)]
36. Rohloff, J. Monoterpene Composition of Essential Oil from Peppermint (*Mentha × piperita* L.) with Regard to Leaf Position Using Solid-Phase Microextraction and Gas Chromatography/Mass Spectrometry Analysis. *J. Agric. Food Chem.* **1999**, *47*, 3782–3786. [[CrossRef](#)] [[PubMed](#)]
37. Menary, R.C.; Garland, S.M. *Authenticating Essential Oil Flavours and Fragrances*; Rural Industries Research and Development Corporation: Kingston, Australia, 1999.
38. Schmidt, E.; Bail, S.; Buchbauer, G.; Stoilova, I.; Atanasova, T.; Stoyanova, A.; Krastanov, A.; Jirovetz, L. Chemical Composition, Olfactory Evaluation and Antioxidant Effects of Essential Oil from *Mentha × piperita*. *Nat. Prod. Commun.* **2009**, *4*, 1934578X0900400819. [[CrossRef](#)]
39. Sadowska, U.; Matwijczuk, A.; Niemczynowicz, A.; Drózdź, T.; Żabiński, A. Spectroscopic Examination and Chemometric Analysis of Essential Oils Obtained from Peppermint Herb (*Mentha piperita* L.) and Caraway Fruit (*Carum carvi* L.) Subjected to Pulsed Electric Fields. *Processes* **2019**, *7*, 466. [[CrossRef](#)]
40. Kucharska-Ambrożej, K.; Martyna, A.; Karpińska, J.; Kiełtyka-Dadasiewicz, A.; Kubat-Sikorska, A. Quality control of mint species based on UV-VIS and FTIR spectral data supported by chemometric tools. *Food Control* **2021**, *129*, 108228. [[CrossRef](#)]
41. Zhang, J.; Li, M.; Zhang, H.; Pang, X. Comparative investigation on aroma profiles of five different mint (*Mentha*) species using a combined sensory, spectroscopic and chemometric study. *Food Chem.* **2022**, *371*, 131104. doi:10.1016/j.foodchem.2021.131104. [[CrossRef](#)]
42. Ragonese, C.; Sciarone, D.; Grasso, E.; Dugo, P.; Mondello, L. Enhanced resolution of *Mentha piperita* volatile fraction using a novel medium-polarity ionic liquid gas chromatography stationary phase. *J. Sep. Sci.* **2016**, *39*, 537–544. [[CrossRef](#)]
43. Dimandja, J.M.D.; Stanfill, S.B.; Grainger, J.; Patterson, D.G., Jr. Application of Comprehensive Two-Dimensional Gas Chromatography (GC×GC) to the Qualitative Analysis of Essential Oils. *J. High Resol. Chromatogr.* **2000**, *23*, 208–214. [[CrossRef](#)]
44. Sang, J. Estimation of menthone, menthofuran, menthyl acetate and menthol in peppermint oil by capillary gas chromatography. *J. Chromatogr. A* **1982**, *253*, 109–112. [[CrossRef](#)]
45. Sivropoulou, A.; Kokkini, S.; Lanaras, T.; Arsenakis, M. Antimicrobial activity of mint essential oils. *J. Agric. Food Chem.* **1995**, *43*, 2384–2388. [[CrossRef](#)]
46. Moghaddam, M.; Pourbaige, M.; Tabar, H.K.; Farhadi, N.; Hosseini, S.M.A. Composition and Antifungal Activity of Peppermint (*Mentha piperita*) Essential Oil from Iran. *J. Essent. Oil Bear. Plants* **2013**, *16*, 506–512. [[CrossRef](#)]
47. Krieger, R. *Handbook of Pesticide Toxicology*; Academic Press: Cambridge, MA, USA, 2001.
48. Khanna, R.; Macdonald, J.K.; Levesque, B.G. Peppermint oil for the treatment of irritable bowel syndrome: A systematic review and meta-analysis. *J. Clin. Gastroenterol.* **2014**, *48*, 505–512. [[CrossRef](#)] [[PubMed](#)]
49. Haber, S.L.; El-Ibiary, S.Y. Peppermint oil for treatment of irritable bowel syndrome. *Am. J. Health Syst. Pharm.* **2016**, *73*, 22–31. [[CrossRef](#)] [[PubMed](#)]
50. Pittler, M.; Ernst, E. Peppermint oil for irritable bowel syndrome: A critical review and metaanalysis. *Am. J. Gastroenterol.* **1998**, *93*, 1131–1135. [[CrossRef](#)]

51. Keifer, D.; Ulbricht, C.; Abrams, T.; Basch, E.; Giese, N.; Giles, M.; Kirkwood, C.; Miranda, M.; Woods, J. Peppermint (*Mentha × piperita*): An evidence-based systematic review by the Natural Standard Research Collaboration. *J. Herb. Pharmacother.* **2007**, *7*, 91–143. [[CrossRef](#)]
52. Kligler, B.; Chaudhary, S. Peppermint oil. *Am. Fam. Physician* **2007**, *75*, 1027–1030.
53. Chumpitazi, B.; Kearns, G.; Shulman, R. Review article: The physiological effects and safety of peppermint oil and its efficacy in irritable bowel syndrome and other functional disorders. *Aliment. Pharmacol. Ther.* **2018**, *47*, 738–752. [[CrossRef](#)]
54. Schmitz, D.; Shubert, V.A.; Betz, T.; Schnell, M. Multi-resonance effects within a single chirp in broadband rotational spectroscopy: The rapid adiabatic passage regime for benzonitrile. *J. Mol. Spectrosc.* **2012**, *280*, 77–84. [[CrossRef](#)]
55. Fatima, M.; Pérez, C.; Arenas, B.E.; Schnell, M.; Steber, A.L. Benchmarking a new segmented K-band chirped-pulse microwave spectrometer and its application to the conformationally rich amino alcohol isoleucinol. *Phys. Chem. Chem. Phys.* **2020**, *22*, 17042–17051. [[CrossRef](#)]
56. Plusquellic, D.F.; Suenram, R.D.; Maté, B.; Jensen, J.O.; Samuels, A.C. The conformational structures and dipole moments of ethyl sulfide in the gas phase. *J. Chem. Phys.* **2001**, *115*, 3057–3067. [[CrossRef](#)]
57. Western, C.M. PGOPHER: A program for simulating rotational, vibrational and electronic spectra. *J. Quant. Spectrosc. Radiat. Transf.* **2017**, *186*, 221–242. [[CrossRef](#)]
58. Pickett, H.M. The Fitting and Prediction of Vibration-Rotation Spectra with Spin Interactions. *J. Mol. Spectrosc.* **1991**, *148*, 371–377. [[CrossRef](#)]
59. Neese, F. The ORCA program system. *Wiley Interdiscip. Rev. Comput. Mol. Sci.* **2012**, *2*, 73–78. [[CrossRef](#)]
60. Neese, F. Software update: The ORCA program system, version 4.0: Software update. *Wiley Interdiscip. Rev. Comput. Mol. Sci.* **2017**, *8*, e1327. [[CrossRef](#)]
61. Grimme, S. Density functional theory with London dispersion corrections. *WIREs Comput. Mol. Sci.* **2011**, *1*, 211–228. [[CrossRef](#)]
62. Schmitz, D.; Shubert, V.A.; Betz, T.; Schnell, M. Exploring the conformational landscape of menthol, menthone, and isomenthone: A microwave study. *Front. Chem.* **2015**, *3*, 15. [[CrossRef](#)]
63. Krin, A.; Pinacho, P.; Pérez, C.; Schnell, M. Menthyl acetate. A new link in the chain of acetates studied with rotational spectroscopy. *J. Mol. Struct.* **2022**, *1252*, 132075. [[CrossRef](#)]
64. Neill, J.L.; Pate, B.H.; Evangelisti, L.; Seifert, N.; Spada, L. Chiral Analysis in Complex Sample Mixtures by Fourier Transform Molecular Rotational Resonance Spectroscopy. In Proceedings of the CPAC Spring Meeting, Seattle, WA, USA, 2–3 May 2016.
65. Moreno, J.R.A.; Huet, T.R.; González, J.J.L. Conformational relaxation of S-(+)-carvone and R-(+)-limonene studied by microwave Fourier transform spectroscopy and quantum chemical calculations. *Struct. Chem.* **2013**, *24*, 1163–1170. [[CrossRef](#)]
66. Neeman, E.; Moreno, J.; Huet, T. The gas phase structure of α -pinene, a main biogenic volatile organic compound. *J. Chem. Phys.* **2017**, *147*, 214305. [[CrossRef](#)]
67. Neeman, E.M.; Avilés-Moreno, J.R.; Huet, T.R. The quasi-unchanged gas-phase molecular structures of the atmospheric aerosol precursor β -pinene and its oxidation product nopinone. *Phys. Chem. Chem. Phys.* **2017**, *19*, 13819–13827. [[CrossRef](#)]
68. Medcraft, C.; Schnell, M. A Comparative Study of Two Bicyclic Ethers, Eucalyptol and 1,4-Cineole, by Broadband Rotational Spectroscopy. *Z. Phys. Chem.* **2015**, *230*, 1–14. [[CrossRef](#)]
69. Kisiel, Z.; Desyatnyk, O.; Białkowska-Jaworska, E.; Pszczółkowski, L. The structure and electric dipole moment of camphor determined by rotational spectroscopy. *Phys. Chem. Chem. Phys.* **2003**, *5*, 820–826. [[CrossRef](#)]
70. Schmitz, D.; Shubert, V.A.; Patterson, D.; Krin, A.; Schnell, M. Phase Dependence of Double-Resonance Experiments in Rotational Spectroscopy. *J. Phys. Chem. Lett.* **2015**, *6*, 1493–1498. [[CrossRef](#)]
71. Pérez, C.; Steber, A.L.; Domingos, S.R.; Krin, A.; Schmitz, D.; Schnell, M. Coherent Enantiomer-Selective Population Enrichment Using Tailored Microwave Fields. *Angew. Chem. Int. Ed.* **2017**, *56*, 12512–12517. [[CrossRef](#)] [[PubMed](#)]
72. Kraitchman, J. Determination of Molecular Structure from Microwave Spectroscopic Data. *Am. J. Phys.* **1953**, *21*, 17–24. [[CrossRef](#)]